mathematics

Article

Traveling Wave Solutions for Complex Space-Time Fractional Kundu-Eckhaus Equation

Mohammed Alabedalhadi [1], Mohammed Shqair [2,*], Shrideh Al-Omari [3] and Mohammed Al-Smadi [1,4,5]

1 Department of Applied Science, Ajloun College, Al-Balqa Applied University, Ajloun 26816, Jordan
2 College of Science, Zarqa University, Zarqa 132222, Jordan
3 Department of Mathematics, Faculty of Science, Al-Balqa Applied University, Ajloun 26816, Jordan
4 Nonlinear Dynamics Research Center (NDRC), Ajman University, Ajman 20550, United Arab Emirates
5 College of Commerce and Business, Lusail University, Doha 122104, Qatar
* Correspondence: mshqair@zu.edu.jo

Abstract: In this work, the class of nonlinear complex fractional Kundu-Eckhaus equation is presented with a novel truncated M-fractional derivative. This model is significant and notable in quantum mechanics with good-natured physical characteristics. The motivation for this paper is to construct new solitary and kink wave solutions for the governing equation using the ansatz method. A complex-fractional transformation is applied to convert the fractional Kundu-Eckhaus equation into an ordinary differential equations system. The equilibria of the corresponding dynamical system will be presented to show the existence of traveling wave solutions for the governing model. A novel kink and solitary wave solutions of the governing model are realized by means of the proposed method. In order to gain insight into the underlying dynamics of the obtained solutions, some graphical representations are drawn. For more illustration, several numerical applications are given and analyzed graphically to demonstrate the ability and reliability of the method in dealing with various fractional engineering and physical problems.

Keywords: fractional Kundu-Eckhaus equation; solitary wave; kink wave; truncated M-fractional derivative

MSC: 81T10; 35J10

Citation: Alabedalhadi, M.; Shqair, M.; Al-Omari, S.; Al-Smadi, M. Traveling Wave Solutions for Complex Space-Time Fractional Kundu-Eckhaus Equation. *Mathematics* **2023**, *11*, 404. https://doi.org/10.3390/math11020404

Academic Editor: Victor Orlov

Received: 15 November 2022
Revised: 25 December 2022
Accepted: 28 December 2022
Published: 12 January 2023

1. Introduction

Quantum mechanics, the core of modern physics, emerged after classical mechanics failed to explain many physical problems, including the Compton effect, photoelectric effect, special relativity, black-body radiation, magnetism, and stability of atoms. These explanations depend on the fact that the quantities are not continuous but are represented by discrete values, which is a new concept of quantization. Quantization is the fundamental building on which quantum mechanics rests. Further, quantum mechanics is a generalization of classical physics that can be applied at the atomic and ordinary levels. The Kundu-Eckhaus equation is an important quantum mechanics equation with good-natured physical properties, which has many applications in various fields of science [1]. Studying the Kundu-Eckhaus equation with the aid of fractional derivatives provides the opportunity for a better understanding of some phenomena in quantum physics, including fractal fibers, nonlinear optics, shallow water propagation, and plasma, while the use of fractional calculus in the quantitative trend is a recent creative topic.

Fractional quantum mechanics is based on the use of a quantum mechanical path integration approach, while non-fractional quantum mechanics uses the Schrödinger wave-function or dynamics of the Heisenberg matrix that arose to get congruence in quantum theory with Lagrange's approach to classical mechanics. In this orientation, quantum mechanics is influenced by Lagrangian and the least-action principle observed by Dirac. This idea is further refined and developed by Feynman, later called a path integral approach, which with the help of the perturbation technique, is used in all fields of modern physics. In [2], the author presented properties for the fractional Schrodinger equation. While in [3], the author studied the fractional quantum via a new path integral technique. The authors of [4] considered an effective analytical method to construct numerical solutions for the fractional resonant Schrödinger model. Finally, solitary and kink wave solutions for the Schrödinger model have been obtained in [5].

The nonlinear fractional Schrödinger equation, especially the fractional Kundu-Eckhaus equation, utilizes space and time derivatives in fractional order instead of second-order space derivatives and first-order time derivatives of the non-fractional standard formula. For this respect, the Schrödinger equation of fractional order is simply a complex fractional partial differential equation according to the modern nomenclature of quantum theories. In the limit of integer case, the fundamental equation of fractional quantum mechanics is transformed into the well-known equation of standard quantum mechanics used to understand in more detail the advanced methods applied in treating fractional problems arising in physics and engineering. The fractional Schrödinger equation has been obtained using a fractional Klein-Gordon equation in [6]. The authors of [7] presented a numerical method to obtain numerical solutions of the fractional system in Hilbert space. In [8], the Schrodinger equation has been considered with a Coulomb potential and solved in fractional space. The authors of [9] considered the fractional Schrödinger equation in Caputo-Fabrizio fractional operator sense and presented a new fractional operator [9]. The computational technique has been presented and utilized in [10]. Coupled Fractional Traveling Wave Solutions of the Extended Boussinesq–Whitham–Broer–Kaup-Type Equations with Variable Coefficients and Fractional Order are introduced in [11].

The main motivation for this study is to construct a new kink and solitary wave solution for the following space-time fractional Kundu-Eckhaus equation (FKEE):

$$i_i\mathcal{D}^{\eta,\,\alpha}_{M,t}g +_i \mathcal{D}^{2\eta,\,\alpha}_{M,x}g - 2a_1\left|g^2\right|g + a_2^2\left|g^4\right|g + 2ia_2g\mathcal{D}^{\eta,\,\alpha}_{M,x}\left(\left|g^2\right|\right) = 0, \quad (1)$$

where a_1 and a_2 are nonzero real constants. Here, g is a complex-valued function of two independent variables x and t that demonstrate the wave profile, i is the imaginary unit, and $\mathcal{D}^{\eta,\,\alpha}_{M}$ is the truncated M-fractional derivative of order η in terms of space-time direction such that $0 < \eta \leq 1$.

Recently, numerous mathematical methods in the literature have been developed to obtain more options for closed-form solutions for fractional models in various branches of physics, which will enrich the mathematical simulation of nature with a deeper understanding and clearer explanation of the influence of fractional operators on the geometrical and physical behavior of solutions. On this occasion, some of these methods have been applied to find accurate and approximate solutions to the nonlinear complex Kundu-Eckhaus equation; for example, in [12], the Q-homotopy analysis transform method has been successfully employed to solve both the Kundu-Eckhaus model and massive Thirring model of fractional order in quantum field theory. At the same time, the modified F-expansion technique has been applied to obtain numerous exact and soliton wave solutions on the nonlinear fractional Kundu-Eckhaus model [13]. Al-Smadi et al. [14] used the conformable residual power series method in handling the approximate solution for the fractional Kundu-Eckhaus model. In [15], the extended sinh-Gordon equation expansion method has been implemented to obtain new closed-form soliton solutions for the Kundu-Eckhaus equation. The exact traveling wave solutions for nonlinear dynamics of microtubules on a model of the Kundu-Eckhaus equation are given in [16]. The optical solutions of the Kundu-Eckhaus equation have been provided by using a new auxiliary equation method [17]. Wang et al. [18] solved the quantic Kundu-Eckhaus equation with the Raman effect in the non-uniform management systems by the similarity transformation method. Optical soliton and rogue wave solutions of ultra-short femto second pulses represented by the Kundu-Eckhaus equation in optical fiber were introduced using two different methods [19]. We aim in this paper to obtain new solitary and kink solitary wave solutions for the space-time FKEE that are considered in a truncated M-fractional derivative sense. The proposed method has not been utilized before, as we know to construct wave solutions for the governing model. Moreover, we introduce the equilibria classification for the FKEE that ensures the existence of the desired solitary and kink wave solutions. We will discuss the effect of the fractional derivative on the behavior of the wave solutions that will be constructed.

The remainder of this paper is arranged as follows: In Section 2, we recall some needed concepts and definitions of the truncated M-fractional derivative. In Section 3, we utilize the proposed complex transformation on the governing model, and we show the existence of traveling wave solutions for it. Section 4 is devoted to constructing kink and solitary wave solutions using the proposed approach. Finally, a simple conclusion remark is pointed out in Section 5.

2. The Truncated M-Fractional Derivative

In recent years, fractional differentiation operators have received the attention of many researchers to study mathematical models related to the functions of complex variables because they are more influential and comprehensive than classical ones while analyzing and interpreting the individual prediction and entire models' behavior [20–28]. We present in this section the definition of the truncated M-fractional derivative and its essential properties that will be useful in this paper.

Definition 1 [29]. *The truncated Mittag-Leffer function having one parameter is stated as follows:*

$$E_\alpha^i(z) = \sum_{n=0}^{i} \frac{z^n}{\Gamma(\alpha n + 1)}, \tag{2}$$

where $\alpha > 0$ *and* $z \in \mathbb{C}$.

Definition 2 [29]. *Let* $u : [0, \infty) \to \mathbb{R}$. *Then the truncated M-fractional derivative of the function* u *of order* η *is acquainted as follows:*

$$_i\mathcal{D}_M^{\eta,\alpha}(u(\zeta)) = \lim_{\epsilon \to 0} \frac{u(\zeta E_\alpha^i(\epsilon \zeta^{1-\eta})) - u(\zeta)}{\epsilon}, \ \forall \zeta > 0, \tag{3}$$

where $0 < \eta < 1$ *and* $\alpha > 0$. *If a truncated M-fractional derivative of the function* u *of order* η *exists, then the function* u *is* η*-differentiable.*

Theorem 1 [29]. *Let* $0 < \eta \leq 1, \alpha > 0, c_1, c_2 \in \mathbb{R}$ *and let the functions* u *and* v *be* η*-differentiable at a point* $\zeta > 0$. *Then the following are satisfied:*

(i)
$$_i\mathcal{D}_M^{\eta,\alpha}(c_1 u + c_2 v)(\zeta) = c_1 {}_i\mathcal{D}_M^{\eta,\alpha}(u(\zeta)) + c_2 {}_i\mathcal{D}_M^{\eta,\alpha}(v(\zeta)). \tag{4}$$

(ii)
$$_i\mathcal{D}_M^{\eta,\alpha}(u.v)(\zeta) = u(\zeta) {}_i\mathcal{D}_M^{\eta,\alpha}(v(\zeta)) + v(\zeta) {}_i\mathcal{D}_M^{\eta,\alpha}(u(\zeta)). \tag{5}$$

(iii)
$$_i\mathcal{D}_M^{\eta,\alpha}\left(\frac{u}{v}\right)(\zeta) = \frac{v(\zeta) {}_i\mathcal{D}_M^{\eta,\alpha}(u(\zeta)) - u(\zeta) {}_i\mathcal{D}_M^{\eta,\alpha}(u(\zeta))}{(v(\zeta))^2}. \tag{6}$$

(iv)
$$_i\mathcal{D}_M^{\eta,\alpha}(c) = 0, \text{ where } u(\zeta) = c \text{ is constant.} \tag{7}$$

(v)
$$\begin{gathered}\text{If the function } u \text{ is differentiable, then :} \\ _i\mathcal{D}_M^{\eta,\alpha}(u(\zeta)) = \frac{\zeta^{1-\eta}}{\Gamma(\alpha+1)} \frac{du(\zeta)}{d\zeta}.\end{gathered} \tag{8}$$

3. Existence of Traveling Wave Solutions of the Space-Time FKEE

The space-time FKEE is an important case of the fractional nonlinear Schrödinger equation. In general, the wave function $g(t,x)$ cannot have a direct physical meaning because it contains a complex quantity, but the multiplication of this wave function and its conjugate $g^*(t,x,)$ gives a real value called the probability density (probability per unit volume) of the particle at a certain position and time [30–32]. To obtain an exact solution of FKEE (1), we use the following complex transformation

$$g(x,t) = \mathcal{G}(\varpi)e^{i\psi},\ \varpi = \frac{ik\Gamma(\alpha+1)(x^\eta - 2\mu t^\eta)}{\eta},\ \psi = \frac{\Gamma(\alpha+1)(\mu x^\eta + \sigma t^\eta)}{\eta}, \tag{9}$$

where μ and σ represent the wave number and wave frequency, respectively. Moreover, by substituting (9) into FKEE (1), we can get the following integer-order ordinary differential equation (ODE):

$$a_2^2\mathcal{G}^5 - 2a_1\mathcal{G}^3 - \left(\mu^2+\sigma\right)\mathcal{G} + 4a_2k\mathcal{G}^2\frac{d\mathcal{G}}{d\varpi} - k^2\frac{d^2\mathcal{G}}{d\varpi^2} = 0. \tag{10}$$

Consequently, the integer-order ODE (10) corresponds to the following dynamical system:

$$\frac{d\mathcal{G}}{d\varpi} = \mathcal{F},$$
$$\frac{d\mathcal{F}}{d\varpi} = \frac{1}{k^2}\left(a_2^2\mathcal{G}^5 - 2a_1\mathcal{G}^3 - \left(\mu^2+\sigma\right)\mathcal{G} + 4a_2k\mathcal{G}^2\mathcal{F}\right). \tag{11}$$

The existence of traveling wave solutions for the governing model (1) consorts with the existence of periodic, homoclinic, and heteroclinic orbits for the dynamical system (11), see [33–35]. Moreover, the periodic orbits consort with periodic wave solutions for the governing model (1), while the homoclinic and heteroclinic orbits consort with solitary and kink wave solutions for (1), respectively. Therefore, we look to determine the equilibrium points for system (11), then we will depict its phase plane to show the corresponding orbits in the $(\mathcal{G},\ \mathcal{F})$-plane. $E(0,0)$ is an equilibrium point for system (11). If we define $f(\mathcal{G}) = a_2^2\mathcal{G}^4 - 2a_1\mathcal{G}^2 - (\mu^2+\sigma)$, then $E(0,\mathcal{G}^*)$ is an equilibrium point for the system (11) provided $\mathcal{G}^*$ is a real root of the function $f(\mathcal{G})$. Therefore, we obtain the following:

Case 1. *If $a_2 \neq 0$ and $\sigma > -\mu^2$, then system (11) has three equilibrium points, namely, $E(0,0)$ and $E(\mathcal{G}_1^\pm,\ 0)$, where $\mathcal{G}_1^\pm = \pm\sqrt{\frac{a_1+\sqrt{a_1^2+a_2^2(\mu^2+\sigma)}}{a_2^2}}$.*

Case 2. *If $a_2 \neq 0,\ a_1 > 0,\ \sigma < 0,\ \mu \leq |\sigma|$ and $\left(-\sqrt{\frac{-a_1^2}{\mu^2+\sigma}} < a_2 < 0 \text{ or } 0 < a_2 < \sqrt{\frac{-a_1^2}{\mu^2+\sigma}}\right)$, then system (11) has five equilibrium points, namely, $E(0,0),\ E(\mathcal{G}_1^\pm,\ 0)$ and $E(\mathcal{G}_2^\pm,\ 0)$, where $\mathcal{G}_1^\pm = \pm\sqrt{\frac{a_1+\sqrt{a_1^2+a_2^2(\mu^2+\sigma)}}{a_2^2}}$ and $\mathcal{G}_2^\pm = \pm\sqrt{\frac{a_1-\sqrt{a_1^2+a_2^2(\mu^2+\sigma)}}{a_2^2}}$.*

Case 3. *If $a_2 = 0$ and $a_1(\mu^2+\sigma) < 0$, then system (11) has three equilibrium points: $E(0,0)$, $E\left(\sqrt{\frac{-(\mu^2+\sigma)}{2a_1}},0\right)$ and $E\left(-\sqrt{\frac{-(\mu^2+\sigma)}{2a_1}},0\right)$.*

Let $M(\mathcal{G},\ \mathcal{F})$ be the coefficient matrix for the linearized system (11), we have:

$$M(\mathcal{G},\ \mathcal{F}) = \begin{bmatrix} 0 & 1 \\ \frac{1}{k^2}\left(5a_2^2\mathcal{G}^4 - 6a_1\mathcal{G}^2 - (\mu^2+\sigma) + 8a_2k\mathcal{G}\mathcal{F}\right) & \frac{4a_2\mathcal{G}^2}{k} \end{bmatrix}. \tag{12}$$

Consider $J(\mathcal{G},\ \mathcal{F}) = \det M(\mathcal{G},\ \mathcal{F})$, then we get:

$$J(\mathcal{G},\ \mathcal{F}) = -\frac{1}{k^2}\left(5a_2^2\mathcal{G}^4 - 6a_1\mathcal{G}^2 - \left(\mu^2+\sigma\right) + 8a_2k\mathcal{G}\mathcal{F}\right). \tag{13}$$

Consequently, we obtain the following:

$$J(E(0,0)) = \frac{\mu^2+\sigma}{k^2}. \tag{14}$$

$$J\left(E\left(\mathcal{G}_1^{\pm},\ 0\right)\right) = -\frac{4\left(a_1^2 + a_2^2(\mu^2+\sigma) + a_1\sqrt{a_1^2 + a_2^2(\mu^2+\sigma)}\right)}{a_2^2k^2}. \tag{15}$$

$$J\left(E\left(\mathcal{G}_2^{\pm},\ 0\right)\right) = -\frac{4\left(a_1^2 + a_2^2(\mu^2+\sigma) - a_1\sqrt{a_1^2 + a_2^2(\mu^2+\sigma)}\right)}{a_2^2k^2}. \tag{16}$$

By the theory of the planner dynamical system, an equilibrium point of system (11) is a center if $J > 0$, while it is a saddle if $J < 0$. Therefore, upon results in (14)–(15), the classifications of the equilibrium points for system (11) depend on the parameters μ, σ, and k. The potential function $P(\mathcal{G})$ for system (11) satisfies the following [36,37]:

$$\frac{d^2\mathcal{G}}{d\varpi^2} = -\frac{dP}{d\mathcal{G}}. \tag{17}$$

Therefore, we obtain the following ODE using (17) and system (11):

$$\frac{d\mathcal{P}}{d\mathcal{G}} = \frac{-1}{k^2}\left(a_2^2\mathcal{G}^5 - 2a_1\mathcal{G}^3 - \left(\mu^2+\sigma\right)\mathcal{G} + 4a_2k\mathcal{G}^2\mathcal{F}\right). \tag{18}$$

Integrate both sides of (18) with respect to $\mathcal{G}$, the potential function $P(\mathcal{G})$ can be given as:

$$\mathcal{P}(\Psi) = \frac{-1}{k^2}\left(\frac{a_2^2}{6}\mathcal{G}^6 - \frac{1}{2}a_1\mathcal{G}^4 - \frac{(\mu^2+\sigma)}{2}\mathcal{G}^2 + \frac{4}{3}a_2k\mathcal{G}^3\mathcal{F}\right). \tag{19}$$

The equilibrium points for system (11) correspond with the extreme points of the potential function $P(\mathcal{G})$ in (19), where the maxima of the potential function correspond to a saddle point for (11), while the minima of the potential function correspond to a center point for (11), see [38]. Figure 1 shows the phase portrait for system (11) and the potential function $P(\mathcal{G})$ in (19). Taking into consideration the selected parameters that satisfy the conditions in case 2, we obtain five equilibrium points, namely, $E(0,0)$ is a saddle, $E(\pm 2.7,0)$ centers and $E(\pm 0.73,0)$ is saddles too. The absolute maxima at P_1 and P_2 of the potential function $P(\mathcal{G})$ shown in Figure 1b correspond with the saddle points $E(\pm 2.7,0)$, while the local maxima at P_0 correspond with the saddle point $E(0,0)$. Moreover, the minima of the potential function $P(\mathcal{G})$ at P_3 and P_4 correspond with the centers $E(\pm 0.73,0)$. We observe that there are two heteroclinic orbits in Figure 1a. The first one starts from $E(2.7,0)$ and connects to $E(0.73,0)$, while the other one starts from $E(-2.7,0)$ and connects to $E(0.73,0)$, which implies the existence of kink wave solutions for (1).

Figure 2 shows the existence of three equilibrium points $E(0,0)$ and $E(\pm 1.73,0)$ which are center and saddle points, respectively. The absolute minima of the potential function $P(\mathcal{G})$ at P_0 correspond with the center $E(0,0)$ for system (11), while the saddle points $E(\pm 1.73,0)$ of system (11) correspond with the local maxima P_1 and P_2.

In Figure 3, we depicted the phase portrait for system (11) that shows three equilibrium points, $E(0,0)$ is a saddle point and $E(\pm 0.7,0)$ is a center. These points correspond to the extreme points for the potential function $P(\mathcal{G})$ that is presented in Figure 3b. We observe the existence of two homoclinic orbits starting from $E(0,0)$ where one of them surrounds the center $E(0.7,0)$ and the other one surrounds the center $E(-0.7,0)$, which implies the existence of solitary wave solutions for (1). In addition, there are periodic orbits surrounding the center $E(\pm 0.7, 0)$.

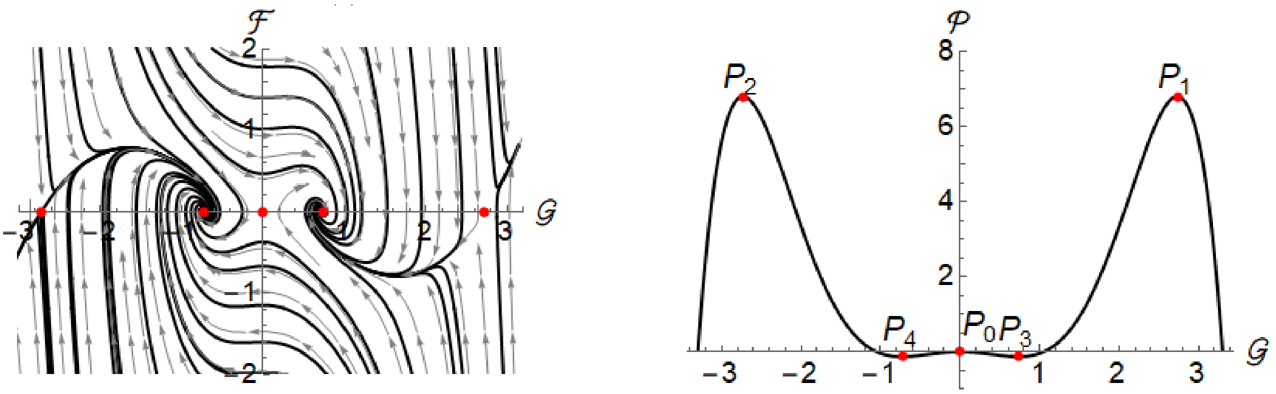

(**a**) (**b**)

Figure 1. Phase portrait for system (11) at $a_1 = 1$, $a_2 = -0.5$, $\sigma = -2$, $\mu = 1$ and $k = 1$ where: (**a**) phase portrait; (**b**) potential function $P(\mathcal{G})$.

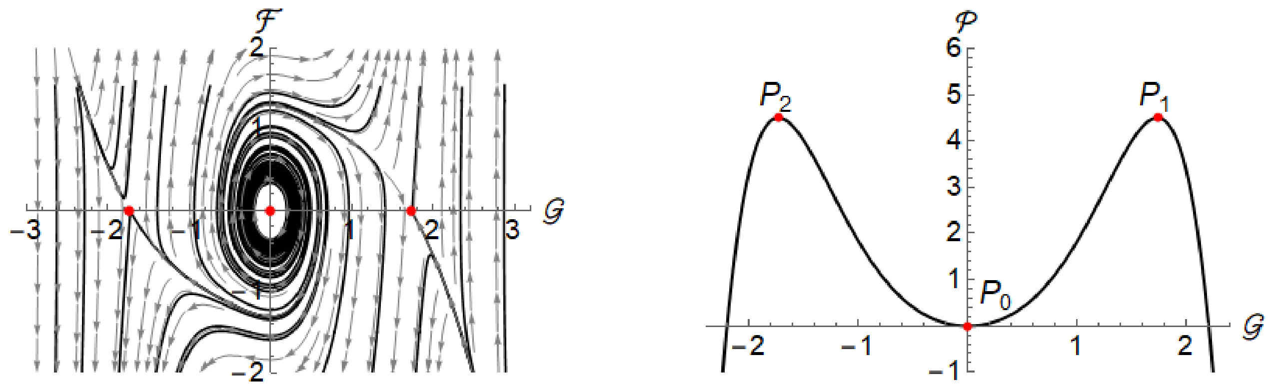

(**a**) (**b**)

Figure 2. Phase portrait for system (11) at $a_1 = 1$, $a_2 = 1$, $\sigma = 2$, $\mu = 1$, and $k = 1$ where: (**a**) phase portrait; (**b**) potential function $P(\mathcal{G})$.

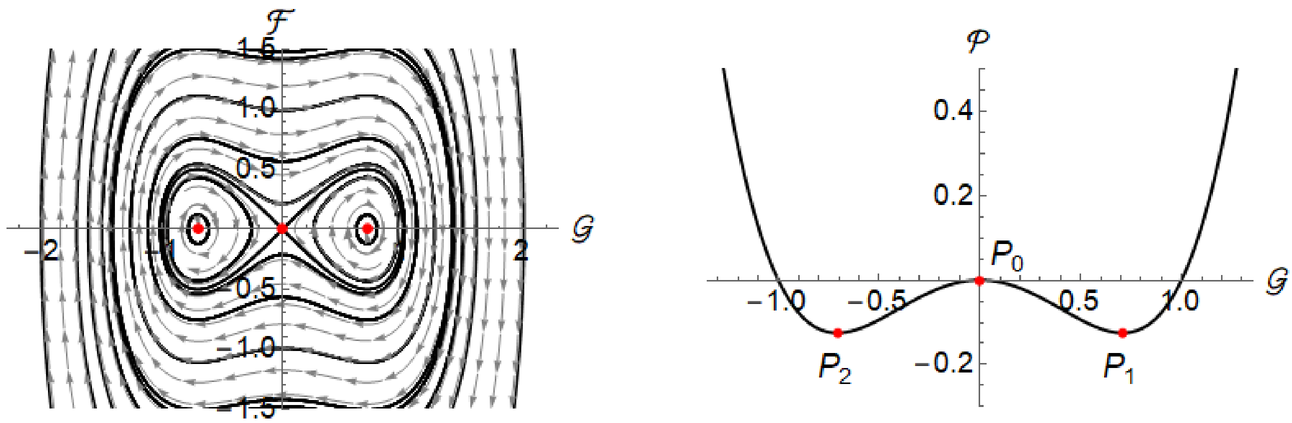

(**a**) (**b**)

Figure 3. Phase portrait for system (11) at $a_1 = 1$, $a_2 = 0$, $\sigma = -2$, $\mu = 1$ and $k = 1$ where: (**a**) phase portrait; (**b**) potential function $P(\mathcal{G})$.

If $a_1 = -1$ and $\sigma = 2$, then it satisfies the conditions in case 3, which implies the existence of three equilibrium points $E(0,0)$ is the center, $E(\pm 1.22, 0)$ is a saddle point for system (11), and these equilibrium points correspond to the minima P_0 and the maxima P_1, P_2, respectively, see Figure 4. Moreover, there are two heteroclinic orbits connecting the saddle points $E(\pm 1.22, 0)$, which implies the existence of kink wave solutions for the governing Equation (1).

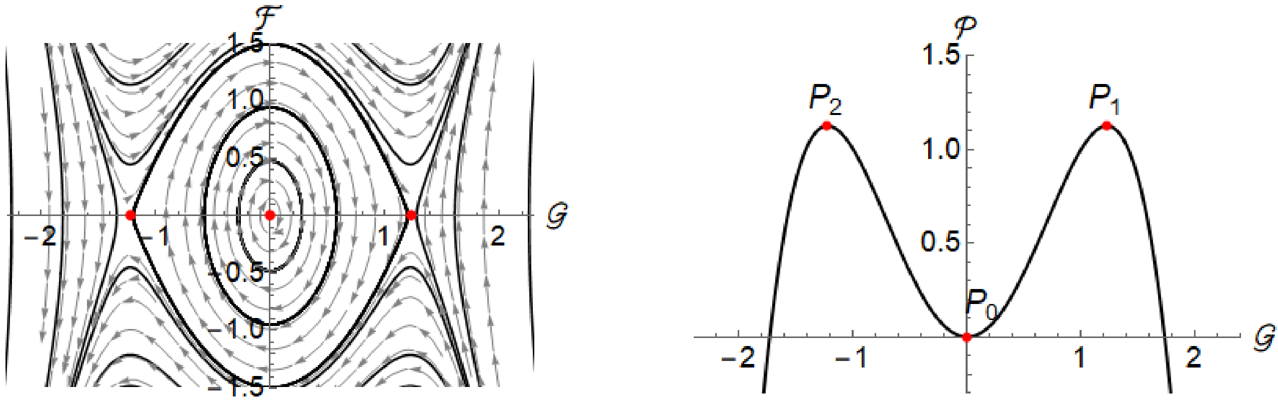

(**a**) (**b**)

Figure 4. Phase portrait for system (11) at $a_1 = -1$, $a_2 = 0$, $\sigma = 2$, $\mu = 1$ and $k = 1$ where: (**a**) phase portrait; (**b**) potential function $P(\mathcal{G})$.

4. Traveling Wave Solutions of the Space-Time FKEE

In this section, we try to construct traveling wave solutions for the space-time FKEE (1) using the ansatz method that considers the solution of the integer-order ODE (10), which can be written as an expression involving hyperbolic functions.

4.1. Kink Wave Solutions

To develop kink wave solutions for the space-time FKEE (1), we consider the solution of the integer-order ODE (10) which can be represented in two formulas involving the hyperbolic function $\tanh(.)$.

4.1.1. First Formula

The solution of the integer-order ODE (10) can be represented as:

$$\mathcal{G}(\varpi) = \Pi_1 \tanh(\Pi_2 \varpi), \tag{20}$$

where Π_1 and Π_2 are constants to be determined. By substituting the expression (20) into the integer-order ODE (10) and, after some simplification, by setting the coefficients of the independent terms to be zero, we obtain:

$$a_2 = 0,\ \Pi_1 = \pm\sqrt{\frac{-(\mu^2+\sigma)}{2a_1}},\ \Pi_2 = \pm\sqrt{\frac{-(\mu^2+\sigma)}{2k^2}}, \tag{21}$$

Provided that $(\mu^2 + \sigma) < 0$ and $a_1 > 0$. Consequently, the solution of the integer-order ODE (10) is given as:

$$\mathcal{G}_{K1}(\varpi) = \sqrt{\frac{-(\mu^2+\sigma)}{2a_1}} \tanh\left(\left(\sqrt{\frac{-(\mu^2+\sigma)}{2k^2}}\right)\varpi\right). \tag{22}$$

Upon the obtained solution in (22) and with the aid of the transformation (9), the kink wave solution for the space-time FKEE (1) is given as follows:

$$g_{K1}(x,t) = \sqrt{\frac{-(\mu^2+\sigma)}{2a_1}}\tanh\left(\left(\sqrt{\frac{-(\mu^2+\sigma)}{2k^2}}\right)\frac{ik\Gamma(\alpha+1)(x^\eta - 2\mu t^\eta)}{\eta}\right)\times e^{i\left(\frac{\Gamma(\alpha+1)(\mu x^\eta+\sigma t^\eta)}{\eta}\right)}. \quad (23)$$

Figure 5a shows the behavior of the obtained kink wave solution (22) at $a_1 = 1$, $k = 1$, $\mu = 1$ and, $\sigma = -2$. In Figure 5b, we present the effect of the wave frequency σ on the behavior of (22).

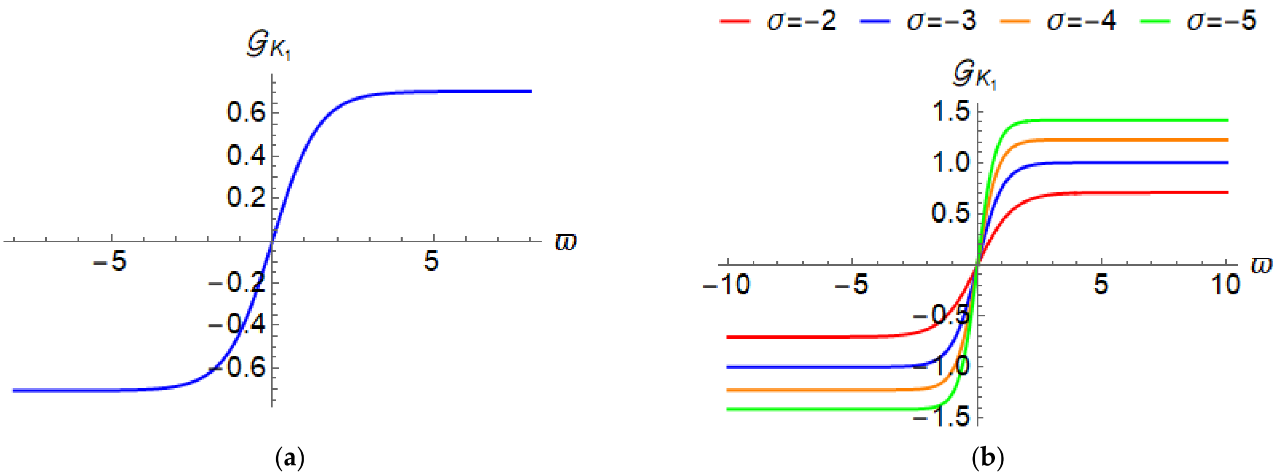

Figure 5. The behavior of kink wave solution $\mathcal{G}_{K1}(\varpi)$ in (22) at $a_1 = 1$, $k = 1$, $\mu = 1$ and the frequency: (**a**) $\sigma = -2$; (**b**) $\sigma = -2, -3, -4$ and -5.

The surface of the obtained kink wave solution is depicted in Figure 6, at $a_1 = 1$, $k = 1$, $\mu = 1$, $\sigma = -10$, $\alpha = 1$ and $\eta = 1$ whereas Figure 6a shows the 3D plot of $|g_{K_1}(x,t)|^2$ in (23) on $(x,t) \in [-2,2] \times [0,1]$, and the 2D plot of $|g_{K_1}(x,0)|^2$ is presented in Figure 6b. The effect of the fractional derivative η studied and the results are presented in Figure 7.

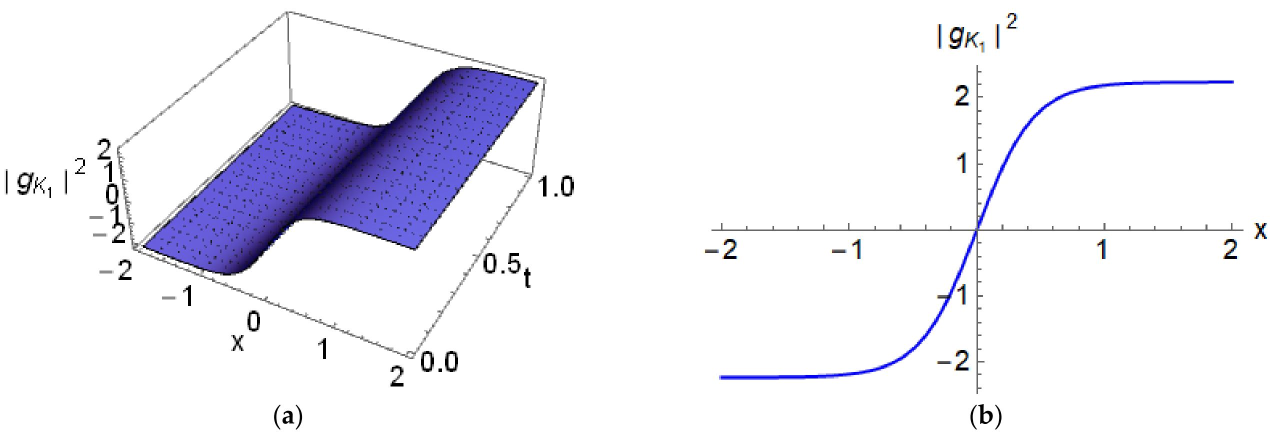

Figure 6. The kink wave solution $|g_{K_1}(x,t)|^2$ in (23) at $a_1 = 1$, $k = 1$, $\mu = 1$, $\sigma = -10$, $\alpha = 1$ and $\eta = 1$ where: (**a**) 3D plot; (**b**) 2D plot at $t = 0$.

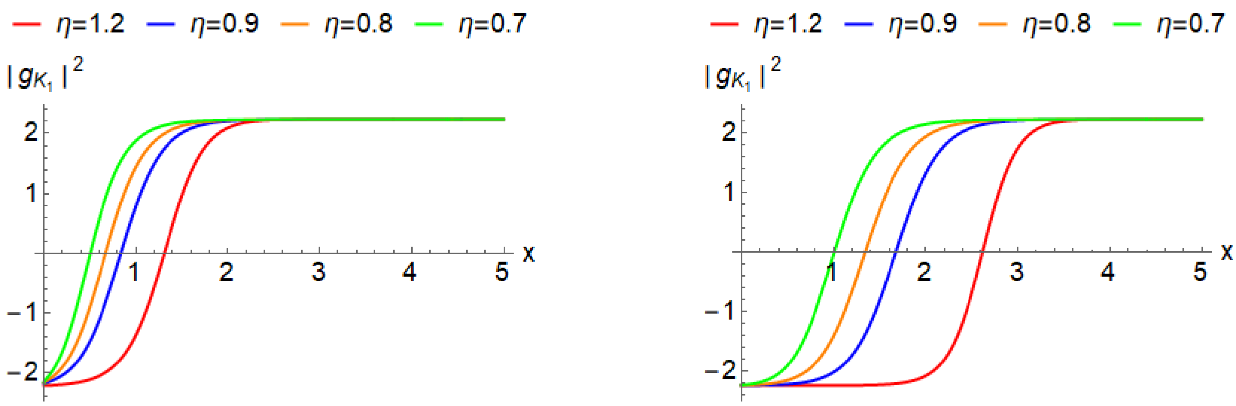

(**a**) (**b**)

Figure 7. Effect of the fractional derivative on the behavior of kink wave solution $|g_{K_1}(x,t)|^2$ in (23) at $a_1 = 1,\ k = 1,\ \mu = 1,\ \sigma = -10,\ \alpha = 1$ where: (**a**) $t = 5$; (**b**) $t = 10$.

4.1.2. Second Formula

The solution of the integer-order ODE (10) can be represented as:

$$\mathcal{G}(\varpi) = \Pi_1 \sqrt{1 + \tanh(\Pi_2 \varpi)}, \tag{24}$$

where Π_1 and Π_2 are constants to be determined. By substituting the expression (24) into the integer-order ODE (10) and, after some simplification, setting the coefficients of the independent terms to be zero, we obtain:

$$\Pi_1 = \pm\sqrt{-\frac{3(\mu^2+\sigma)}{a_1} \pm \frac{\sqrt{7}\sqrt{a_1^2(\mu^2+\sigma)^2}}{a_1^2}}, \tag{25}$$

$$\Pi_2 = \pm\sqrt{\frac{-(\mu^2+\sigma)}{k^2}}, \tag{26}$$

$$a_2 = \frac{\Pi_1^2 a_1 + \mu^2 + \sigma}{2\Pi_1^2 \Pi_2 k}. \tag{27}$$

Provided that $\mu^2 + \sigma < 0$ and $a_1 > 0$. Consequently, the solutions of the integer-order ODE (10) are given as:

$$\mathcal{G}_{K_2}^{\pm}(\varpi) = \pm\sqrt{\frac{-3a_1(\mu^2+\sigma) \pm \sqrt{7\left(a_1^2(\mu^2+\sigma)^2\right)}}{a_1^2}} \sqrt{1 + \tanh\left(\left(\pm\sqrt{\frac{-(\mu^2+\sigma)}{k^2}}\right)\varpi\right)}. \tag{28}$$

Upon the obtained solutions in (28) with the aid of the transformation (9), then the kink wave solutions for the space-time FKEE (1) are given as follows:

$$\begin{aligned} g_{K_2}^{\pm}(x,t) = &\pm\left(\sqrt{\frac{-3a_1(\mu^2+\sigma) \pm \sqrt{7\left(a_1^2(\mu^2+\sigma)^2\right)}}{a_1^2}}\right. \\ &\times\left.\sqrt{1 + \tanh\left(\left(\pm\sqrt{\frac{-(\mu^2+\sigma)}{k^2}}\right)\frac{ik\Gamma(\alpha+1)(x^\eta - 2\mu t^\eta)}{\eta}\right)}\right) \\ &\times e^{i\left(\frac{\Gamma(\alpha+1)(\mu x^\eta + \sigma t^\eta)}{\eta}\right)}. \end{aligned} \tag{29}$$

Figure 8a shows the behavior of the obtained kink wave solution (22) at $a_1 = 1$, $k = 1$, $\mu = 1$ and $\sigma = -2$. In Figure 5b, we present the effect of the wave frequency σ on the behavior of (22).

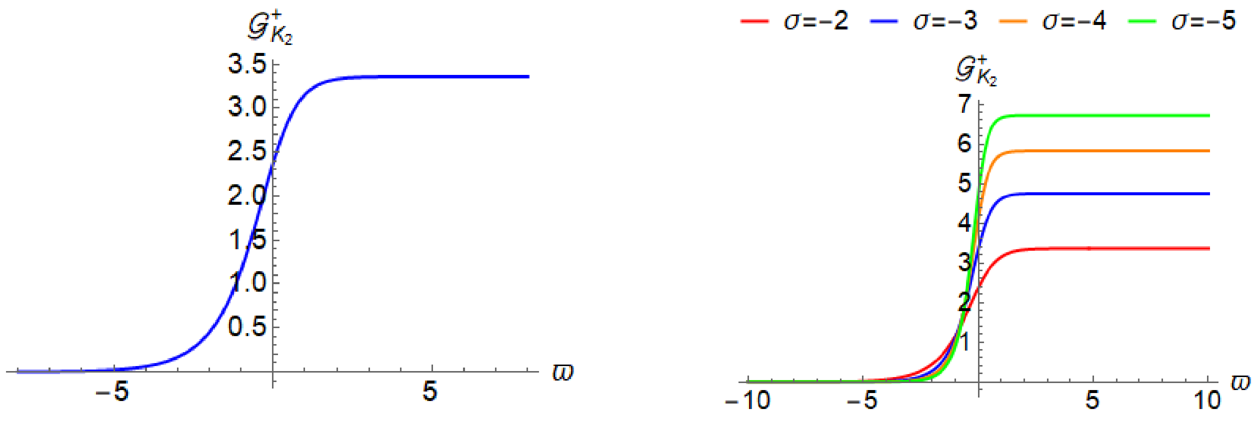

Figure 8. The behavior of kink wave solution $\mathcal{G}^{+}_{K_2}(\varpi)$ in (28) at $a_1 = 1$, $k = 1$, $\mu = 1$ and the frequency: (**a**) $\sigma = -2$; (**b**) $\sigma = -2, -3, -4$ and -5.

In Figure 9, we present 3D and 2D plots for the constructed kink wave solution $\left|g^{-}_{K_2}(x,t)\right|^2$ in (29) at $a_1 = 1$, $k = 1$, $\mu = 1$, $\sigma = -10$, $\alpha = 1$ and $\eta = 1$ on $(x,t) \in [-2,2] \times [0,1]$.

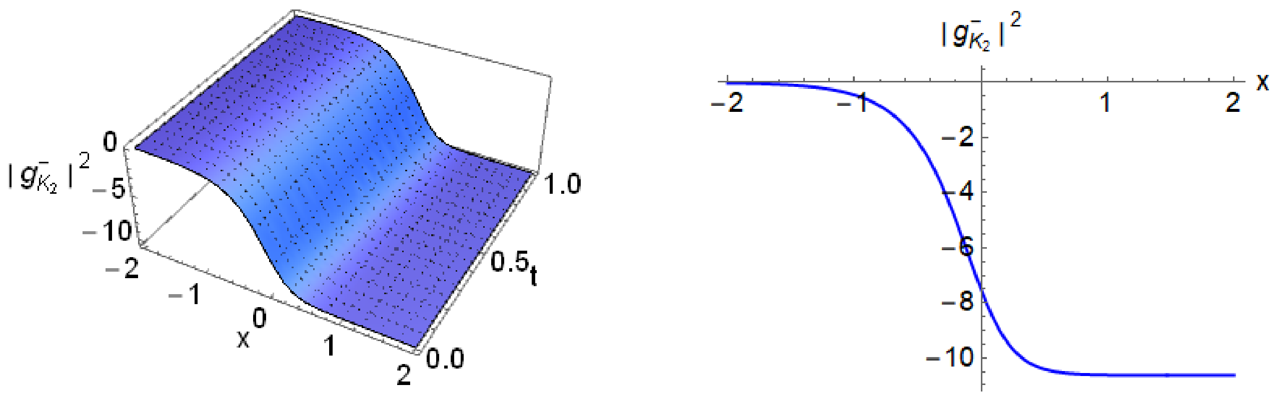

Figure 9. The kink wave solution $\left|g^{-}_{K_2}(x,t)\right|^2$ in (29) at $a_1 = 1$, $k = 1$, $\mu = 1$, $\sigma = -10$, $\alpha = 1$ and $\eta = 1$ where: (**a**) 3D plot; (**b**) 2D plot at $t = 0$.

The fractional derivative affects the behavior of the developed kink wave solution on (29). To illustrate this effect, we show a 2D plot of $\left|g^{+}_{K_1}(x,t)\right|^2$ in (29) at different fractional derivative orders where the time is $t = 10$ and $t = 20$ in Figure 10a and b, respectively.

4.2. Solitary Wave Solutions

The solitary wave solutions for the governing model (1) will be constructed using two formulas involving the hyperbolic functions $\sec h(.)$ and $\cosh(.)$.

4.2.1. First Formula

Here, we consider the solution of the integer-order ODE (10) can be represented as:

$$\mathcal{G}(\varpi) = \Pi_1 \sec h(\Pi_2 \varpi), \tag{30}$$

where Π_1 and Π_2 are constants to be determined. By substituting the expression (30) into the integer-order ODE (10) and, after some simplification, setting the coefficients of the independent terms to be zero, we obtain:

$$a_2 = 0,\ \Pi_1 = \pm\sqrt{\frac{-(\mu^2+\sigma)}{a_1}},\ \Pi_2 = \pm\sqrt{\frac{-(\mu^2+\sigma)}{k^2}}. \tag{31}$$

Provided that $\mu^2 + \sigma < 0$ and $a_1 > 0$. Consequently, the solutions of the integer-order ODE (10) are given:

$$\mathcal{G}^{\pm}_{S_1}(\varpi) = \pm\sqrt{\frac{-(\mu^2+\sigma)}{a_1}}\,\mathrm{sec\,h}\left(\left(\pm\sqrt{\frac{-(\mu^2+\sigma)}{k^2}}\right)\varpi\right). \tag{32}$$

Upon the obtained solutions in (32) with the aid of the transformation (9), then the solitary wave solutions for the space-time FKEE (1) are given as follows:

$$g^{\pm}_{S_1}(x,t) = \pm\sqrt{\frac{-(\mu^2+\sigma)}{a_1}}\,\mathrm{sec\,h}\left(\left(\pm\sqrt{\frac{-(\mu^2+\sigma)}{k^2}}\right)\frac{ik\Gamma(\alpha+1)(x^\eta - 2\mu t^\eta)}{\eta}\right)\times e^{i\left(\frac{\Gamma(\alpha+1)(\mu x^\eta + \sigma t^\eta)}{\eta}\right)}. \tag{33}$$

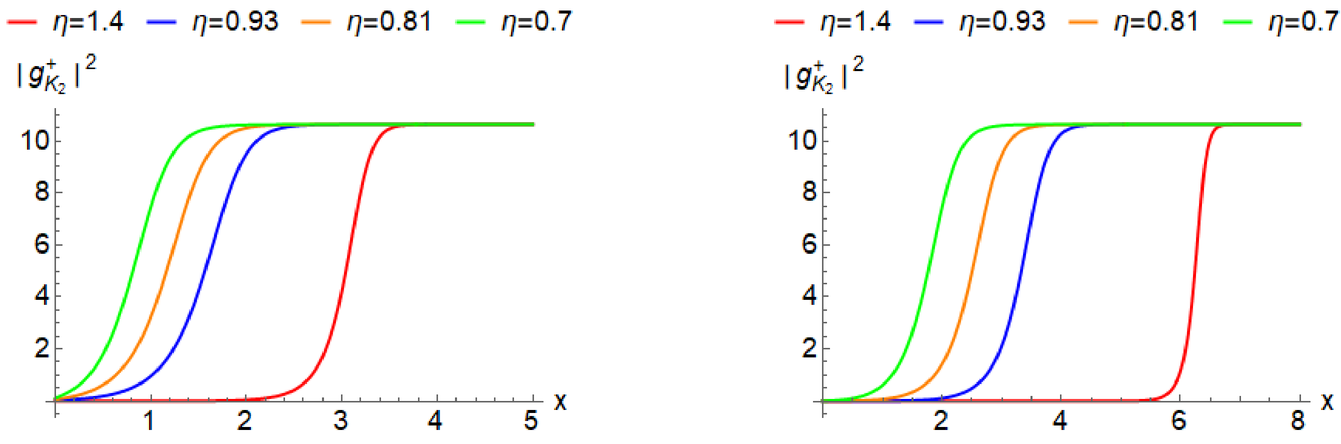

Figure 10. Effect of the fractional derivative on the behavior of kink wave solution $\left|g^{+}_{K_1}(x,t)\right|^2$ in (29) at $a_1 = 1,\ k = 1,\ \mu = 1,\ \sigma = -10,\ \alpha = 1$ where: (**a**) $t = 10$; (**b**) $t = 20$.

Figure 11 presents the solitary wave solution $\mathcal{G}^{+}_{S_1}(\varpi)$ in (32) at $a_1 = 1,\ k = 1,\ \mu = 1$ and $\sigma = -2$. In Figure 11b, we present the effect of the wave frequency σ on the behavior of (22). We note that the decrease in frequency σ corresponds with an increase in the crest of the obtained solitary wave solution.

In Figure 12, we present 3D and 2D plots for the constructed solitary wave solution $\left|g^{+}_{S_1}(x,t)\right|^2$ in (33) at $a_1 = 1,\ k = 1,\ \mu = 1,\ \sigma = -10,\ \alpha = 1$ and $\eta = 1$ on $(x,t) \in [-2,2] \times [0,1]$.

To illustrate the fractional derivative effect on the behavior of the developed kink wave solution on (33), a 2D plot of $\left|g^{+}_{S_1}(x,t)\right|^2$ in (33) at different fractional derivative orders where the time $t = 7$ and $t = 10$ are shown in Figure 13a and b, respectively.

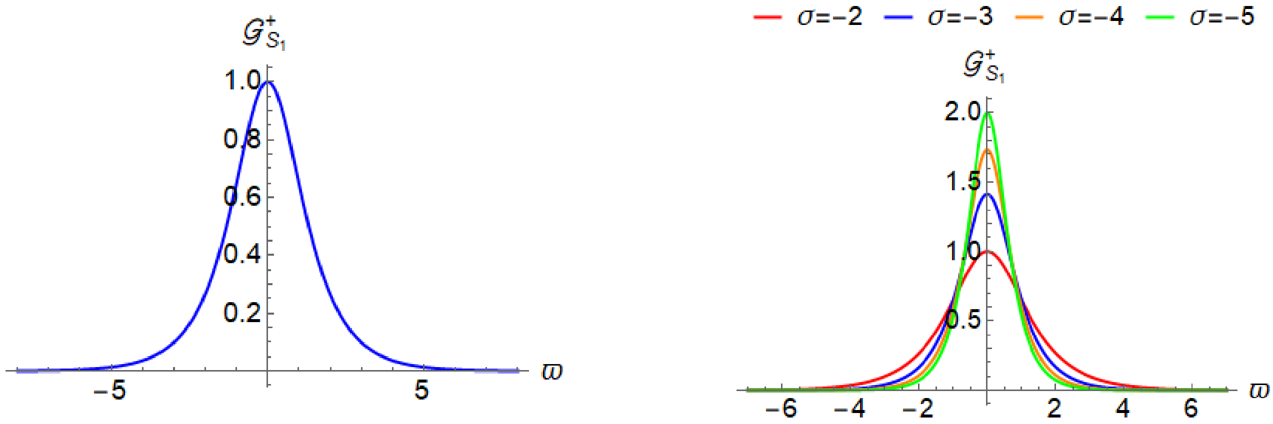

(**a**) (**b**)

Figure 11. The behavior of kink wave solution $\mathcal{G}^{+}_{K_2}(\varpi)$ in (32) at $a_1 = 1$, $k = 1$, $\mu = 1$ and the frequency: (**a**) $\sigma = -2$; (**b**) $\sigma = -2, -3, -4$ and -5.

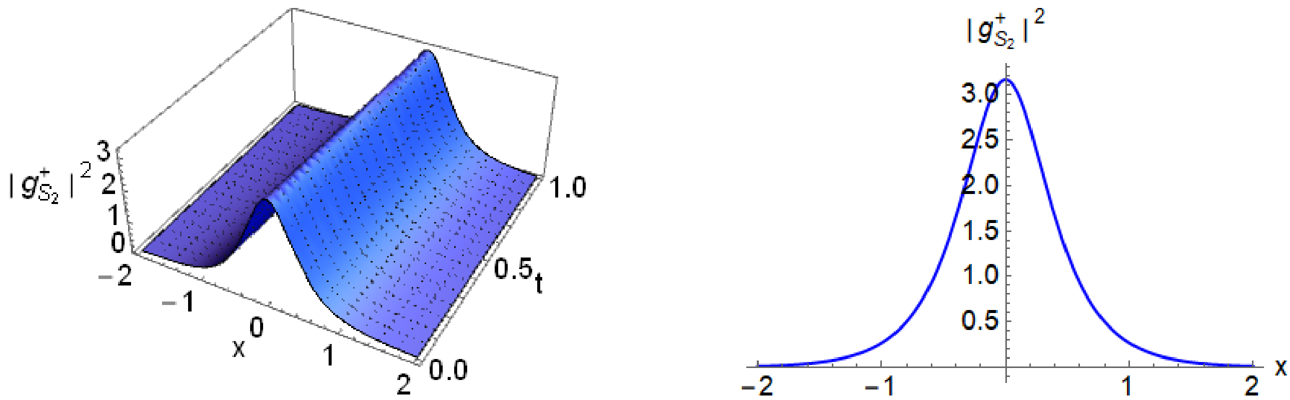

(**a**) (**b**)

Figure 12. The solitary wave solution $\left|g^{+}_{S_1}(x,t)\right|^2$ in (33) at $a_1 = 1$, $k = 1$, $\mu = 1$, $\sigma = -10$, $\alpha = 1$ and $\eta = 1$ where: (**a**) 3D plot; (**b**) 2D plot at $t = 0$.

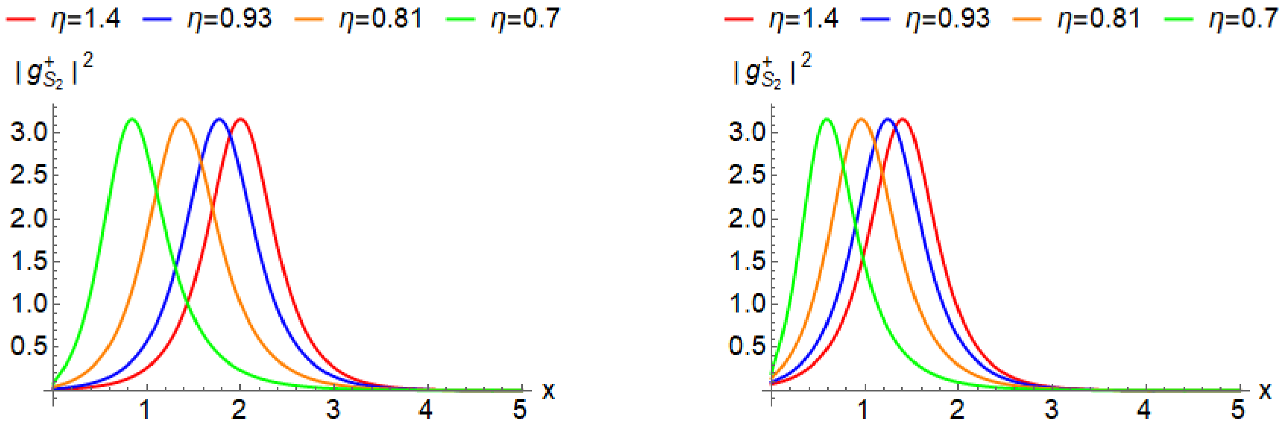

(**a**) (**b**)

Figure 13. Effect of the fractional derivative on the behavior of kink wave solution $\left|g^{+}_{S_1}(x,t)\right|^2$ in (33) at $a_1 = 1$, $k = 1$, $\mu = 1$, $\sigma = -10$, $\alpha = 1$ where: (**a**) $t = 7$; (**b**) $t = 10$.

4.2.2. Second Formula

This formula considered the solution of the integer-order ODE (10) can be represented as:

$$\mathcal{G}(\varpi) = \frac{\Pi_1}{\sqrt{1+\cosh(\Pi_2\varpi)}}, \quad (34)$$

where Π_1 and Π_2 are constants to be determined. By substituting the expression (34) into the integer-order ODE (10) and, after some simplification, setting the coefficients of the independent terms to be zero, we obtain:

$$a_2 = 0,\ \Pi_1 = \pm\sqrt{\frac{-2(\mu^2+\sigma)}{a_1}},\ \Pi_2 = \pm\sqrt{\frac{-4(\mu^2+\sigma)}{k^2}}. \quad (35)$$

Provided that $\mu^2+\sigma<0$ and $a_1>0$. Consequently, the solutions of the integer-order ODE (10) are given:

$$\mathcal{G}^{\pm}_{S_2}(\varpi) = \frac{\pm\sqrt{\frac{-2(\mu^2+\sigma)}{a_1}}}{\sqrt{1+\cosh\left(\left(\pm\sqrt{\frac{-4(\mu^2+\sigma)}{k^2}}\right)\varpi\right)}}. \quad (36)$$

Upon the obtained solutions in (36) with the aid of the transformation (9), then the solitary wave solutions for the space-time FKEE (1) are given as follows:

$$g^{\pm}_{S_1}(x,t) = \frac{\pm\sqrt{\frac{-2(\mu^2+\sigma)}{a_1}}}{\sqrt{1+\cosh\left(\left(\pm\sqrt{\frac{-4(\mu^2+\sigma)}{k^2}}\right)\frac{ik\Gamma(\alpha+1)(x^\eta-2\mu t^\eta)}{\eta}\right)}} \times e^{i\left(\frac{\Gamma(\alpha+1)(\mu x^\eta+\sigma t^\eta)}{\eta}\right)}. \quad (37)$$

Figure 14 presents the solitary wave solution $\mathcal{G}^{+}_{S_2}(\varpi)$ in (36) at $a_1=1,\ k=1,\ \mu=1$, and, $\sigma=-2$. In Figure 14b, we present the effect of the wave frequency σ on the behavior of (36). We note that the decrease in frequency σ corresponds with an increase in the crest of the obtained solitary wave solution.

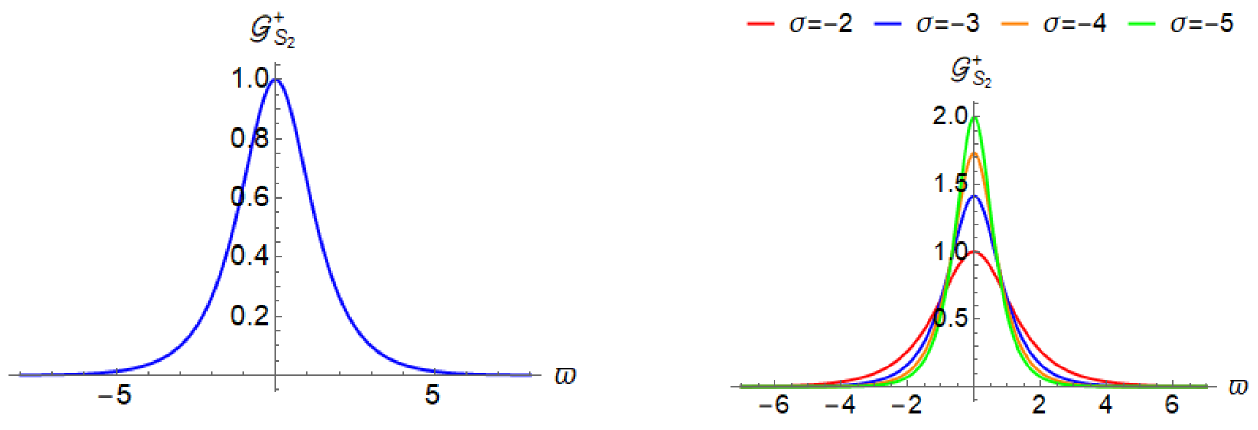

Figure 14. The behavior of kink wave solution $\mathcal{G}^{+}_{K_2}(\varpi)$ in (32) at $a_1=1,\ k=1,\ \mu=1$ and the frequency: (**a**) $\sigma=-2$; (**b**) $\sigma=-2,-3,-4$ and -5.

5. Conclusions

The space-time FKEE is a significant model in quantum optics due to its potential to foretell the ultrashort pulses paths and its usage in the analysis of the properties of the optical. Moreover, the governing model is notable in mechanics due to its role in Stokes waves' sustainability in nonlinear weakly diffusive media. In addition, the space-time FKEE plays a role in the physics of plasma because of its usage to represent ion-acoustic waves. In this work, kink and solitary wave solutions for the space-time fractional Kundu-Eckhaus equation with truncated M-fractional derivative have been determined via the ansatz method. Using complex transformation, the governing model is reduced into integer-order ODE. The equilibria classification was introduced to show the existence of traveling wave solutions. The validity of the proposed method has been tested by implementing it successfully to the space-time fractional KEE for different values of fractional order. In this regard, some graphical representations of the obtained traveling wave solutions have been plotted in 2D and 3D utilizing the Mathematica wolfram computation package. The proposed approach provides a powerful and systematic tool for obtaining novel exact traveling wave solutions and dealing with other nonlinear fractional governing equations arising in mathematical physics, quantum mechanics, and other fields of science.

Author Contributions: Conceptualization, M.A.-S. and S.A.-O.; methodology, M.A.; software, M.A.; validation, M.S., S.A.-O. and M.A.-S.; formal analysis, M.S.; investigation, M.S.; resources, S.A.-O.; data curation, S.A.-O.; writing—original draft preparation, M.A.; writing—review and editing, M.S.; visualization, M.A.-S.; supervision, M.A.-S.; project administration, S.A.-O.; funding acquisition, M.S. All authors have read and agreed to the published version of the manuscript.

Funding: This research is funding by Zarqa university.

Data Availability Statement: Not applicable.

Conflicts of Interest: The authors declare that they have no conflict of interest.

References

1. Griffiths, D.J.; Schroeter, D.F. *Introduction to Quantum Mechanics*; Cambridge University Press: Cambridge, UK, 2018.
2. Laskin, N. Fractional Schrödinger equation. *Phys. Rev. E* **2002**, *66*, 056108. [CrossRef] [PubMed]
3. Laskin, N. Fractional quantum mechanics and Lévy path integrals. *Phys. Lett. A* **2000**, *268*, 298–305. [CrossRef]
4. Al-Smadi, M.; Abu Arqub, O.; Momani, S. Numerical computations of coupled fractional resonant Schrödinger equations arising in quantum mechanics under conformable fractional derivative sense. *Phys. Scr.* **2020**, *95*, 075218. [CrossRef]
5. Alabedalhadi, M.; Al-Smadi, M.; Al-Omari, S.; Baleanu, D.; Momani, S. Structure of optical soliton solution for nonliear resonant space-time Schrödinger equation in conformable sense with full nonlinearity term. *Phys. Scr.* **2020**, *95*, 105215. [CrossRef]
6. Muslih, S.I.; Agrawal, O.P.; Baleanu, D. A fractional Schrödinger equation and its solution. *Int. J. Theor. Phys.* **2010**, *49*, 1746–1752. [CrossRef]
7. Hasan, S.; Al-Smadi, M.; El-Ajou, A.; Momani, S.; Hadid, S.; Al-Zhour, Z. Numerical approach in the Hilbert space to solve a fuzzy Atangana-Baleanu fractional hybrid system. *Chaos Solitons Fractals* **2020**, *143*, 110506. [CrossRef]
8. Eid, R.; Muslih, S.I.; Baleanu, D.; Rabei, E. On fractional Schrödinger equation in α-dimensional fractional space. *Nonlinear Anal. Real World Appl.* **2009**, *10*, 1299–1304. [CrossRef]
9. Gómez-Aguilar, J.F.; Baleanu, D. Schrödinger equation involving fractional operators with non-singular kernel. *J. Electromagn. Waves Appl.* **2017**, *31*, 752–761. [CrossRef]
10. Al-Smadi, M.; Abu Arqub, O. Computational algorithm for solving fredholm time-fractional partial integrodifferential equations of dirichlet functions type with error estimates. *Appl. Math. Comput.* **2019**, *342*, 280–294. [CrossRef]
11. Choi, J.; Kim, H. Coupled Fractional Traveling Wave Solutions of the Extended Boussinesq–Whitham–Broer–Kaup-Type Equations with Variable Coefficients and Fractional Order. *Symmetry* **2021**, *13*, 1396. [CrossRef]
12. Arafa, A.A.M.; Hagag, A.M.S. *Q*-homotopy analysis transform method applied to fractional Kundu-Eckhaus equation and fractional massive Thirring model arising in quantum field theory. *Asian-Eur. J. Math.* **2019**, *12*, 1950045. [CrossRef]
13. Ali, A.; Seadawy, A.R.; Lu, D. Dispersive analytical soliton solutions of some nonlinear waves dynamical models via modified mathematical methods. *Adv. Differ. Equations* **2018**, *2018*, 334. [CrossRef]
14. Al-Smadi, M.; Abu Arqub, O.; Hadid, S. Approximate solutions of nonlinear fractional Kundu-Eckhaus and coupled fractional massive Thirring equations emerging in quantum field theory using conformable residual power series method. *Phys. Scr.* **2020**, *95*, 105205. [CrossRef]
15. Kumar, D.; Manafian, J.; Hawlader, F.; Ranjbaran, A. New closed form soliton and other solutions of the Kundu-Eckhaus equation via the extended sinh-Gordon equation expansion method. *Optik* **2018**, *160*, 159–167. [CrossRef]
16. Khater, M.M.A. Exact traveling wave solutions for nonlinear dynamics of microtubules—A new model and the Kundu-Eckhaus equation. *Commun. Numer. Anal.* **2019**, *2*, 78–90. [CrossRef]
17. Rezazadeh, H.; Korkmaz, A.; Eslami, M.; Mirhosseini-Alizamini, S.M. A large family of optical solutions to Kundu-Eckhaus model by a new auxiliary equation method. *Opt. Quantum Electron.* **2019**, *51*, 84. [CrossRef]

18. Wang, P.; Feng, L.; Shang, T.; Guo, L.; Cheng, G.; Du, Y. Analytical soliton solutions for the cubic–quintic nonlinear Schrödinger equation with Raman effect in the nonuniform management systems. *Nonlinear Dyn.* **2014**, *79*, 387–395. [CrossRef]
19. Khatera, M.M.A.; Seadawy, A.R.; Lua, D. Optical soliton and rogue wave solutions of the ultra-short femto-second pulses in an optical fiber via two different methods and its applications. *Optik* **2018**, *158*, 434–450. [CrossRef]
20. Gao, W.; Veeresha, P.; Prakasha, D.G.; Baskonus, H.M.; Yel, G. New Numerical Results for the Time-Fractional Phi-Four Equation Using a Novel Analytical Approach. *Symmetry* **2020**, *12*, 478. [CrossRef]
21. Baleanu, D.; Fernandez, A. On some new properties of fractional derivatives with Mittag-Leffler kernel. *Commun. Nonlinear Sci. Numer. Simul.* **2018**, *59*, 444–462. [CrossRef]
22. Alruwaili, A.D.; Seadawy, A.R.; Ali, A.; Beinane, S.A.O. Novel Analytical Approach for the Space-Time Fractional (2+1)-Dimensional Breaking Soliton Equation via Mathematical Methods. *Mathematics* **2021**, *9*, 3253. [CrossRef]
23. Baleanu, D.; Machado, J.A.T.; Luo, A.C. (Eds.) *Fractional Dynamics and Control*; Springer: New York, NY, USA, 2012.
24. Ibrahim, R.W.; Baleanu, D. Symmetry Breaking of a Time-2D Space Fractional Wave Equation in a Complex Domain. *Axioms* **2021**, *10*, 141. [CrossRef]
25. Burqan, A.; El-Ajou, A.; Saadeh, R.; Al-Smadi, M. A new efficient technique using Laplace transforms and smooth expansions to construct a series solution to the time-fractional Navier-Stokes equations. *Alex. Eng. J.* **2021**, *61*, 1069–1077. [CrossRef]
26. Shah, N.A.; Rauf, A.; Vieru, D.; Sitthithakerngkiet, K.; Kumam, P. Analytical Solutions of the Diffusion–Wave Equation of Groundwater Flow with Distributed-Order of Atangana–Baleanu Fractional Derivative. *Appl. Sci.* **2021**, *11*, 4142. [CrossRef]
27. Kilbas, A.A.; Srivastava, H.M.; Trujillo, J.J. *Theory and Applications of Fractional Differential Equations*; North-Holland Mathematics Studies; Elsevier: Amsterdam, The Netherlands, 2006; Volume 204.
28. Podlubny, I. *Fractional Differential Equations*; Mathematics in Science and Engineering; Elsevier: Amsterdam, The Netherlands, 1999; Volume 198, pp. 41–119.
29. Sousa, J.V.D.C.; de Oliveira, E.C. A New Truncated M-Fractional Derivative Type Unifying Some Fractional Derivative Types with Classical Properties. *Int. J. Anal. Appl.* **2018**, *16*, 83–96. [CrossRef]
30. Lu, D.Z. Abundant Jacobi elliptic function solutions of nonlinear evolution equations. *Acta Phys. Sin.* **2005**, *54*, 4501–4505.
31. Shqair, M.; Al-Smadi, M.; Momani, S.; El-Zahar, E. Adaptation of conformable residual power series scheme in solving nonlinear fractional quantum mechanics problems. *Appl. Sci.* **2020**, *10*, 890. [CrossRef]
32. Shqair, M.; Alabedalhadi, M.; Al-Omari, S.; Al-Smadi, M. Abundant Exact Travelling Wave Solutions for a Fractional Massive Thirring Model Using Extended Jacobi Elliptic Function Method. *Fractal Fract.* **2022**, *6*, 252. [CrossRef]
33. Hirsch, M.W. Geometrical methods in the theory of ordinary differential equations. *Bull. Am. Math. Soc.* **1984**, *10*, 305–311. [CrossRef]
34. Glushkov, A.V. *Methods of a Chaos Theory*; Astroprint: Odessa, Ukraine, 2012.
35. Verhulst, F. *Nonlinear Differential Equations and Dynamical Systems*; Springer Science & Business Media: Berlin/Heidelberg, Germany, 2006.
36. Freihet, A.; Hasan, S.; Alaroud, M.; Al-Smadi, M.; Ahmad, R.R.; Din, U.K.S. Toward computational algorithm for time-fractional Fokker-Planck models. *Adv. Mech. Eng.* **2019**, *11*, 1687814019881039. [CrossRef]
37. Jharna, T.; Saha, A. Bifurcations of small-amplitude supernonlinear waves of the mKdV and modified Gardner equations in a three-component electron-ion plasma. *Phys. Plasmas* **2020**, *27*, 012105. [CrossRef]
38. Dubinov, A.E.; Kolotkov, D.Y.; Sazonkin, M.A. Nonlinear theory of ion-sound waves in a dusty electron-positron-ion plasma. *Tech. Phys.* **2012**, *57*, 585–593. [CrossRef]